CrystEngComm

Accepted Manuscript

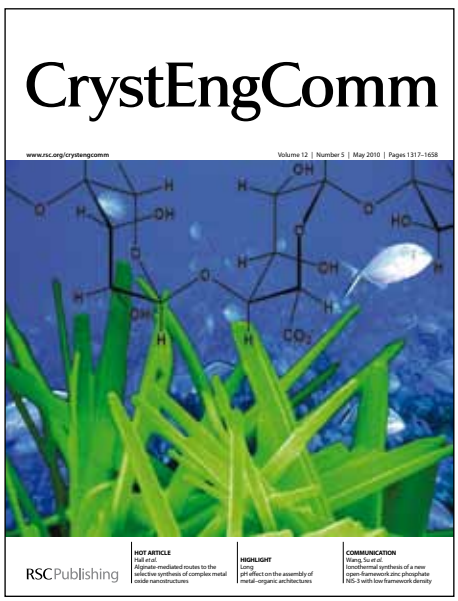

Cite this: DOI: 10.1039/c0xx00000x

www.rsc.org/xxxxxx

ARTICLE TYPE

Deprotonation of Resorcinarenes by Mono- and Diamine Bases: Complexation and Intermolecular Interactions in the Solid State

N. Kodiah Beyeh,[a] Arto Valkonen[a,b] and Kari Rissanen[a]*

Received (in XXX, XXX) Xth XXXXXXXXX 20XX, Accepted Xth XXXXXXXXX 20XX

DOI: 10.1039/b000000x

The deprotonation of resorcinarenes by mono- and dibasic amines, *viz.* triethyl amine (TEA) and its dibasic analogue, *N*,*N*′-dimethyl piperazine (DMPip), was studied and the resulting supramolecular complexes analysed in the solid state, in solution and in the gas phase. In the solid state 1:1 ($2TEAH^+$•(ethyl-resorcinarene)$^{2-}$•MeOH), 3:2 [TEA•$2TEAH^+$•2(ethyl-resorcinarene$^-$)] and 3:2 [2DMPip•$DMPip^{2+}$@(2-Methyl-ethyl-resorcinarene$^-$)$_2$•2MeOH] solid state complexes and interesting resorcinare$^-$···resorcinarene$^-$ supramolecular networks via enhanced hydrogen bonds involving the hydroxyl groups and the deprotonated hydroxyl groups of the resorcinarenes were observed. The host-guest complexes manifest multiple cation···π and C–H···π interactions as in neutral resorcinarene inclusion complexes. The deprotonation of the resorcinarenes were observed in solution through titration studies. In the gas phase, the deprotonation of the resorcinarene and the encapsulation of the resulting ammonium ions were observed in the negative and positive ion modes, respectively.

Introduction

Supramolecular chemistry researchers are in a constant pursuit of designing supramolecular systems that can mimic covalent systems while utilizing a variety of weak interactions.[1,2] A compromise between the competing weak interactions and geometrical constraints is usually the final result making the task of predicting and designing supramolecular architectures based on multiple weak interactions very challenging.[3] The bowl shape cavity of resorcinarenes usually stabilized by four intramolecular hydrogen bonds offers an interesting array of binding modes such as C–H···π and cation···π interactions to recognize a variety of guests.[4-6] The multiple hydroxyl groups can participate in a series of intermolecular hydrogen bonds with guest molecules.[4] This unique cone conformation of resorcinarenes has led to the synthesis of many receptors with convergent arrangement of binding sites suitable for molecular recognition in many applications.[4,7]

Unfunctionalized resorcinarenes are known to easily form molecular complexes with guests of varying shapes and sizes.[6,8] In the presence of suitable guests' species, 1:1 open inclusion complexes,[9,10] capsular[7,11-16] and tubular[17,18] assemblies involving resorcinarenes linked together by hydrogen bonds have been extensively reported. The resulting assembly usually reflects the size and electronic nature of the guests. Small cationic species such as tetramethyl ammonium cation[8,11,15] have the tendency to form dimeric assemblies while larger guest species such as tetrahexyl ammonium salts,[19,20] or pseudo octahedral tris(2,2'-bipyridine)ruthenium(II) salt[16] results in hexameric assemblies.

Understanding non-covalent interactions, steric and topological properties of molecules and building blocks is sometimes an impossible task without the help of crystal engineering.[3,21] Crystal engineering focuses on the design and construction of crystalline solids with desired architectures and functions. Single crystal X-ray crystallography has become one of the main tools in the investigation of supramolecular structures and their interactions in the solid state.[3,21]

Acids and bases have a long history of being constantly used as catalysts in a wide variety of synthetic processes.[22-26] Amines are very common bases used in many catalytic processes.[22] A good example is the use of amines as bases in the alkylation and acylation of resorcinarenes leading to cavitands, carcerands, hemicarcerands and velcrands.[27-30] The use of amines in such reactions is to deprotonate the resorcinarene hydroxyl groups hence facilitating the alkylation and acylation processes.[30-32] However, the isolation and structural characterisation of the deprotonated resorcinarene in such reactions has not been extensively studied. The octa-phenolic hydroxyl groups make resorcinarenes acidic in nature while possessing a π basic cavity. Deprotonation of the phenolic hydroxyl groups will render these compounds anionic in nature, introducing an interesting scenario of intra and intermolecular hydrogen bonds. Only the mono-deprotonated resorcinarene under different conditions have been isolated in the solid state.[33-36] In this contribution, we present several examples of supramolecular assemblies resulting from the deprotonation of resorcinarenes by mono- and dibasic amines, *viz.* triethyl amine, **3** and its dibasic analog, *N*,*N*′-dimethyl piperazine, **4** (Fig. 1). The subsequent protonated ammonium cation then forms interesting supramolecular complexes with the anionic and dianionic resorcinarenes.

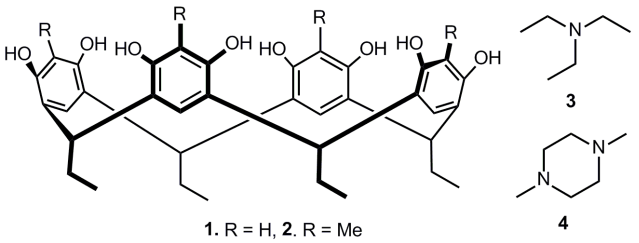

Fig. 1 Resorcinarene **1**-**2**, tertiary monoamine **3** and diamine **4**.

These assemblies are studied in the solid state by single crystal X-ray diffraction studies, in solution by ^{1}H NMR titration analyses and in the gas phase via mass spectrometric analyses.

Results and Discussion

In the crystal structure **I** (2[**3**H]$^+$•[**1**-2H]$^{2-}$•MeOH), the resorcinarene host **1** crystallized out from aqueous MeOH as doubly deprotonated (determination of the deprotonation, see ESI), dianion [**1**-2H]$^{2-}$ with two protonated triethyl amine [**3**H]$^+$ cations and with one MeOH molecule. The structure displays a 1:1 anionic complex {[**1**-2H]$^{2-}$•[**3**H]$^+$}$^-$ with the second protonated amine [**3**H]$^+$ cation (cation B) hydrogen bonded to one of the deprotonated OH groups (phenolate), the solvent MeOH being H-bonded to the same phenolate oxygen as

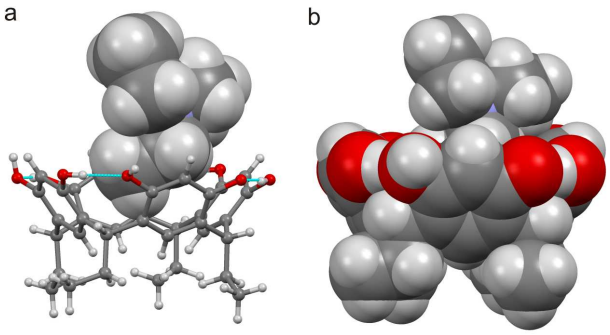

Fig. 2 (a) Ball and stick (cation A in CPK style) and (b) CPK representations of the crystal structure **I** showing one protonated amine [**3**H]$^+$ nicely sitting in the cavity of the doubly deprotonated resorcinarene [**1**-2H]$^{2-}$ forming a 1:1 inclusion anionic complex {[**1**-2H]$^{2-}$•[**3**H]$^+$}$^-$.

the exo-cavity [**3**H]$^+$ cation B. In this 1:1 complex (Fig. 2) the [**3**H]$^+$ cation (cation A) is sitting inside the bowl cavity of the resorcinarene dianion and is hydrogen bonded to the OH group of the adjacent dianion creating a tightly bound dimeric assembly (Figure 3, Table 2). The cavity included cation A shows disorder in all three ethyl groups, which were refined by splitting the methylene groups and methyl protons in two parts with 89:11 ratio.

Table 1 Crystallographic parameters for structures **I** – **III** (CCDC deposition number).

Identification code	**I** (969816)	**II** (969817)	**III** (969818)
Empirical formula	$C_{49}H_{74}N_2O_9$	$C_{45}H_{61}N_3O_8$	$C_{50}H_{73}N_3O_9$
Fw. / gmol^{-1}	835.10	771.97	860.11
T / K	123.0(1)	123.0(1)	173.0(1)
Wavelength / Å	1.54184	1.54184	0.71073
Crystal system	Monoclinic	Triclinic	Triclinic
Space group	$P2_1/n$	P-1	P-1
Unit cell dimensions			
a / Å	11.6120(2)	11.0544(5)	11.7076(5)
b / Å	14.5363(2)	11.9545(5)	14.7176(6)
c / Å	27.4010(4)	17.4371(9)	15.4943(6)
α / °	90	109.915(4)	107.092(2)
β / °	101.0186(14)	100.321(4)	94.407(2)
γ / °	90	97.585(4)	110.946(2)
V / Å^3	4539.90(12)	2084.5(2)	2333.2(2)
Z	4	2	2
ρ_{calc} / Mgm^{-3}	1.222	1.230	1.224
μ / mm^{-1}	0.664	0.675	0.083
F(000)	1816	832	932
Crystal size / mm^3	0.15 × 0.12 × 0.05	0.14 × 0.09 × 0.03	0.28 × 0.25 × 0.12
θ range / °	3.29 – 69.98	3.94 – 69.99	2.29 – 25.00
Index ranges	-14 ≤ h ≤ 13	-13 ≤ h ≤ 12	-13 ≤ h ≤ 13
	-17 ≤ k ≤ 17	-14 ≤ k ≤ 10	-16 ≤ k ≤ 17
	-33 ≤ l ≤ 33	-21 ≤ l ≤ 21	-18 ≤ l ≤ 18
Reflections collected	16003	13473	29369
R_{int}	0.0197	0.0259	0.0804
Completeness to θ / %	99.2	99.4	97.0
Absorption correction	Multi-scan	Multi-scan	Multi-scan
Max. / min. transmission	0.9676 / 0.9070	0.9800 / 0.9114	0.7457 / 0.5847
Data[a] / restraints / parameters	8547 / 105 / 596	7869 / 28 / 538	8194 / 9 / 599
Reflections [I>2σ(I)]	7434	6113	5833
Goodness-of-fit on F^2	1.030	1.050	1.091
Final R indices [I>2σ(I)]	R1 = 0.0383	R1 = 0.0502	R1 = 0.0707
	wR2 = 0.0980	wR2 = 0.1449	wR2 = 0.1485
R indices (all data)	R1 = 0.0451	R1 = 0.0660	R1 = 0.1043
	wR2 = 0.1033	wR2 = 0.1581	wR2 = 0.1660
Largest diff. peak & hole / e.Å^{-3}	0.261 / -0.222	0.394 / -0.343	0.425 / -0.260

[a] Independent reflections.

Cite this: DOI: 10.1039/c0xx00000x

www.rsc.org/xxxxxx

ARTICLE TYPE

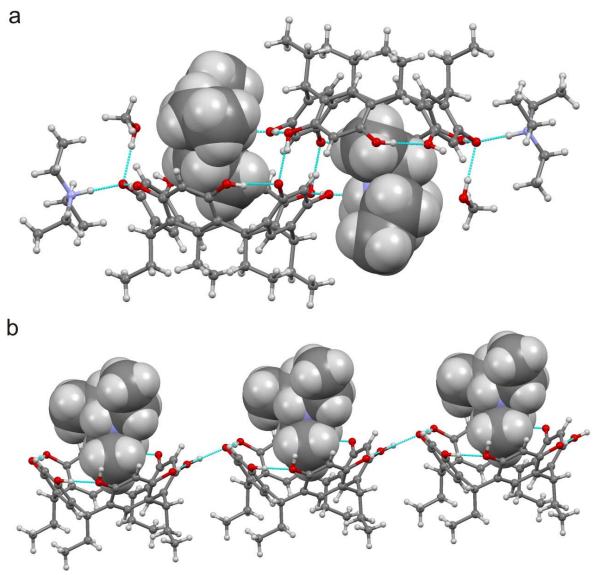

Fig. 3 Ball and stick representation of side-by-side complexes with direct intermolecular hydrogen bond between one deprotonated hydroxyl group of one resorcinarene and a hydroxyl group of a second resorcinarene in opposite (a) and parallel (b) positions in structure **I**. The bound protonated amines are in CPK style.

The two anionic complexes $\{[\mathbf{1}\text{-}2H]^{2-}\bullet[\mathbf{3}H]^{+}\}^{-}$ are very strongly intermolecularly hydrogen bonded to each other via the deprotonated, *viz.* phenolate groups, forming two symmetrical $O^{-}\cdots$H-O H-bonds (O···O 2.54 Å, Fig. 3a). These phenolate oxygens are further hydrogen bonded to an adjacent dianion via another $O^{-}\cdots$H-O hydrogen bonds (also 2.54 Å, Fig. 3b) further extending the network of the dianions along the *a* axis and throughout the crystal. All classical N–H···O and O–H···O hydrogen bonds found from structure **I** are listed in Table 2. As typical for a phenolate hydrogen bond acceptor, both deprotonated O atoms accept three separate hydrogen bonds[37]

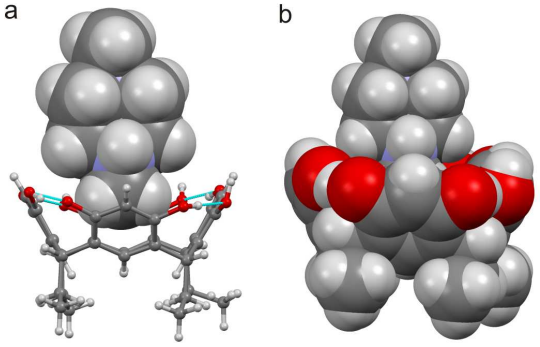

Fig. 4 (a) Ball and stick (cation in CPK style) and (b) CPK representations of the crystal structure **II** showing one protonated amine $[\mathbf{4}H]^{+}$ nicely sitting in the cavity of the singly deprotonated resorcinarene $[\mathbf{1}\text{-}H]^{-}$ forming a 1:1 inclusion complex $[\mathbf{1}\text{-}H]^{-}\bullet[\mathbf{4}H]^{+}$.

one of them accepting three aromatic O-H hydrogen bonds (one intra- and two intermolecular), the other accepts three different hydrogen bonds, one intramolecular aromatic O-H bond, O-H from MeOH and N-H from the exo-cavity $[\mathbf{3}H]^{+}$ cation. As seen from Fig. 3, the cation A is sideways deeply encapsulated into the cavity, but the different orientation and H-bonding to the adjacent dianion, hinders the dimeric capsule formation observed for a very similar but neutral resorcinarene with the same cation but hydrogen bonded to water molecule.[38] These narrow opening between the dimeric dianion assemblies are occupied by the B cations.

In the crystal structure **II** $(3\bullet2[\mathbf{4}H]^{+}\bullet2[\mathbf{1}\text{-}H]^{-})$, the resorcinarene **1** in PrOH/MeCN (1:1) solvent mixture with *N,N′*-dimethyl piperazine as the base yielded a 3:2 overall structure, consisting of two 1:1 inclusion complexes $[\mathbf{1}\text{-}H]^{-}\bullet[\mathbf{4}H]^{+}$ glued together by one non-protonated **4** molecule (the asymmetric unit contains one $[\mathbf{4}H]^{+}$, 0.5 **4** and one resorcinarene). The $[\mathbf{4}H]^{+}$ cation sits deeply in the cavity with the positively charged N atom pointing to bottom of the cavity (Fig. 4).

Table 2 The hydrogen bonding details for structures **I** – **III** (the O…O and N…O distances and O-H…O and N-H…O angles).

	I $d_{D\cdots A}$ / Å, $\angle_{D-H\cdots A}$ / °	**II** $d_{D\cdots A}$ / Å, $\angle_{D-H\cdots A}$ / °	**III** $d_{D\cdots A}$ / Å, $\angle_{D-H\cdots A}$ / °
O(3)-H(3O)...O(2)	2.646(1), 173(2)	2.728(2), 169(3)	2.707(3), 178(4)
O(4)-H(4O)...O(5)	2.670(1), 171(2)	2.625(2), 167(3)	2.703(3), 169(4)
O(6)-H(6O)...O(7)	2.645(1), 178(2)	2.645(2), 176(3)	
O(8)-H(8O)...O(1)	2.679(1), 174(2)	2.656(2), 167(3)	2.691(3), 170(4)
O(7)-H(7O)...O(6)			2.711(3), 167(4)
O(1)-H(1O)...O(5)	2.536(1), 163(2)[a]	2.518(2), 161(3)[b]	
O(1)-H(1O)...O(9)			2.611(3), 173(4)
O(2)-H(2O)...O(6)			2.584(3), 167(4)[a]
O(2)-H(2O)...N(3)		2.649(2), 164(3)[b]	
O(5)-H(5O)...N(2)			2.578(3), 172(4)
O(7)-H(7O)...O(5)	2.543(1), 170(2)[c]	2.541(2), 174(3)[d]	
O(9)-H(9O)...O(2)	2.761(2), 179(2)		
O(9)-H(9O)...N(3)			2.768(4), 163(4)
N(1)-H(1N)...O(6)	2.780(2), 171(2)[c]	2.730(2), 169(2)[d]	2.703(3), 172(3)
N(2)-H(2N)...O(2)	2.613(2), 174(2)		

[a] Symmetry operations: [a] x+1, y, z; [b] x, y+1, z; [c] –x. –y, –z+1; [d] –x, –y+1, –z

Cite this: DOI: 10.1039/c0xx00000x

www.rsc.org/xxxxxx

ARTICLE TYPE

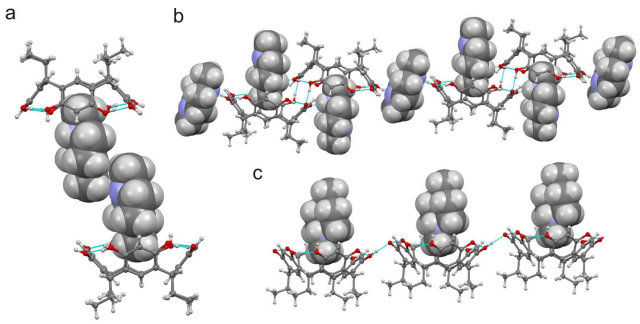

Fig. 5 Ball and stick representation of (a) a dimeric 2x2 assembly 2x{[**1**-H]$^-$•[**4**H]$^+$} through close contact of the protonated amines, (b) a side-by-side complexes with direct intermolecular hydrogen bonds between the deprotonated hydroxyl group of one resorcinarene and a hydroxyl group of a second resorcinarene in opposite directions linked together by the unprotonated diamine, (c) intermolecular hydrogen bonds connecting the anionic hosts in a parallel side-by-side fashion in structure **II**. The protonated and neutral amines are in CPK style.

As in the structure **I**, similar N$^+$–H···O interaction connects the cation to the adjacent resorcinarene anion (Table 2). The free base ends of the two adjacent cations [**4**H]$^+$ show close contact with each other by weak double C–H···N interaction (Fig. 5a). There are also weak C–H···π ($d_{C\cdots}\pi$ = 3.32–3.55 Å) interactions between the cation and the anion found to connect them to each other. The neutral diamine is located around the point of inversion (½,½,½) beside the resorcinarene anion and is accepting two symmetry related O–H···N hydrogen bonds donated by adjacent hosts from opposite directions (Fig. 5b,Table 2). It is also linking the host to the next one (which is upside down due to inversion) by donating C–H···π ($d_{C\cdots}\pi$ = 3.35 Å) and C–H···O ($d_{C\cdots O}$ = 3.23 Å) contacts to two opposite directions.

The resorcinol moieties of host anion in the 1:1 complex [**1**-H]$^-$•[**4**H]$^+$ are also connected to each other with four intramolecular O–H···O hydrogen bonds. The two intermolecular O–H···O interactions connect the anionic hosts with similar opposite (Fig. 5b) and parallel (Fig. 5c) side-by-side fashions as in {[**1**-2H]$^{2-}$•[**3**H]$^+$}$^-$ The anions in opposite positions are connected to each other by a similar double interaction, as in {[**1**-2H]$^{2-}$•[**3**H]$^+$}$^-$ and the parallel fashion is leading to the formation of infinite chains (along *b* axis). As already mentioned, the extra O–H···N hydrogen bonds in the structure **II** (*vs.* structure **I**) connect the anions to cocrystallized diamine molecule. All N–H···O and O–H···O interactions found from structure **II** are listed in Table 2, which show that phenolate oxygen also accepts three O–H···O$^-$ hydrogen bonds.

The 2-methylresorcinarene **2** in aqueous MeOH with diamine **4** resulted in the crystal structure **III**, a formally 3:2 complex [24•[**4**2H]$^{2+}$@([**2**-H]$^-$)$_2$•2MeOH] in which two singly deprotonated resorcinarene [**2**-H]$^-$ hosts encapsulate the doubly protonated [**4**2H]$^{2+}$ dication forming a dimeric pseudo-capsular assembly. The two unprotonated diamines and one MeOH

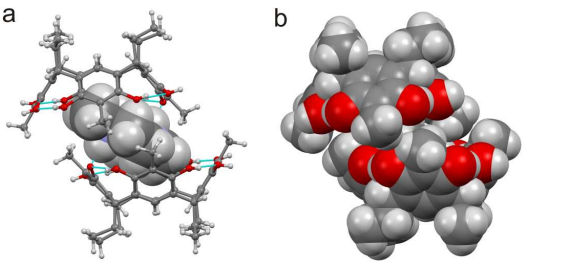

Fig. 6 (a) Ball and stick (cation in CPK style) and (b) CPK representations of the crystal structure **III** showing two singly deprotonated resorcinarenes [**2**-H]$^-$ and one doubly protonated [**4**2H]$^{2+}$ amine forming a dimeric pseudo-capsule [**4**2H]$^{2+}$@([**2**-H]$^-$)$_2$.

molecule are hydrogen bonded to the dimeric pseudo-capsule. The [**4**2H]$^{2+}$ dication is located around the point of inversion (1,1,0) inside the cavity of the pseudo-capsule. The intramolecular N$^+$–H···O$^-$ guest-to-host hydrogen bonds (Table 2) binds the guest between the two halves of the pseudo-capsular [**4**2H]$^{2+}$@([**2**-H]$^-$)$_2$ complex (Fig. 6). This assembly is further reinforced by weaker C–H···O ($d_{C\cdots O}$ = 3.32 Å) and C–H···π ($d_{C\cdots}\pi$ = 3.26–3.52 Å) interactions. The two unprotonated diamines around the point of inversions (0,½,½; ½,½,0) are situated between the resorcinarenes.

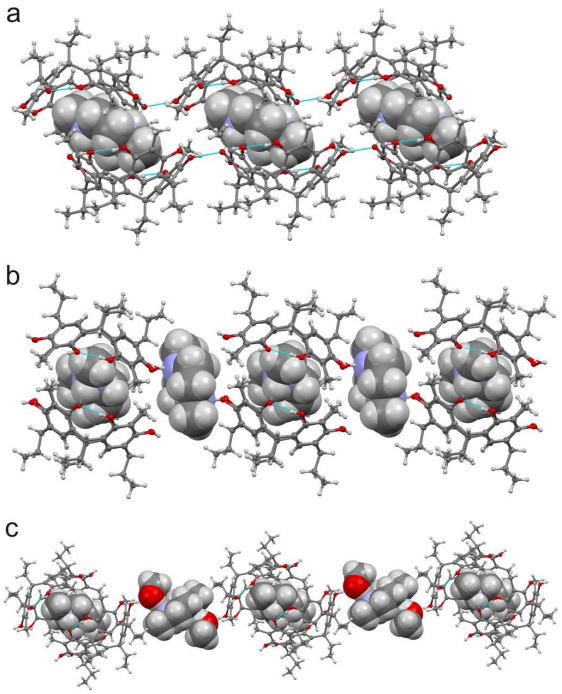

Fig. 7 Ball and stick representation of (a) intermolecular O–H···O$^-$ hydrogen bonds linking the pseudo capsules, (b) O–H···N hydrogen bonds between the host and diamine A molecules leading to the formation of pseudo capsular chains in *ab* plane interlinked by diamine A molecules, (c) intermolecular hydrogen bonds involving hosts, neutral diamines and MeOH molecules creating an infinite chain of pseudo capsules in structure **III**. The protonated and neutral diamines are in CPK style.

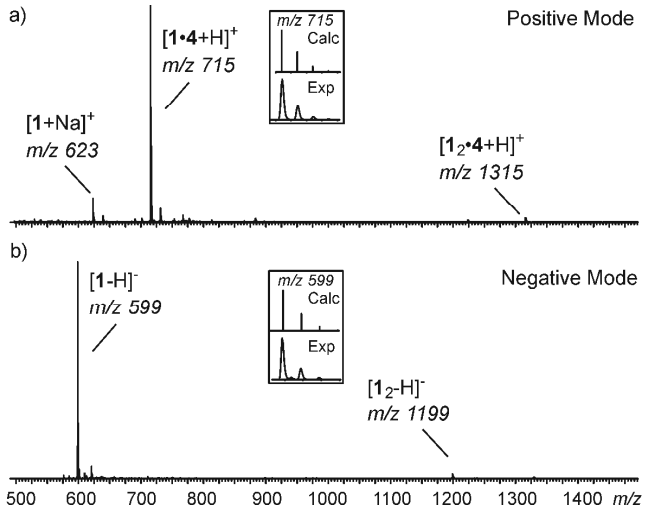

Fig. 8 Electrospray ionization mass spectra of an equimolar mixture of resorcinarene **1** and diamine **4**. (a) Positive ion mode showing the 1:1 monomeric $[\mathbf{1}\bullet\mathbf{4}+H]^+$ *m/z* 715 and dimeric $[\mathbf{1}_2\bullet\mathbf{4}+H]^+$ *m/z* 1315. (b) Negative ion mode showing the deprotonated resorcinarene monomer $[\mathbf{1}-H]^-$ *m/z* 599 and dimer $[\mathbf{1}_2-H]^-$ *m/z* 1199.

The first diamine (diamine A) is bound by the host with direct O–H···N hydrogen bond and the second diamine (diamine B) with MeOH mediated O–H···O–H···N motif (Figures 7b and 7c, Table 2). The Fig. 6 illustrates that the $[\mathbf{4}2H]^{2+}$ dication is clearly encapsulated by two anionic hosts $[\mathbf{2}-H]^-$, but without direct host-host interactions, forming the $[\mathbf{4}2H]^{2+}@([\mathbf{2}-H]^-)_2$ pseudo-capsule.

The host molecule donates a total of seven hydrogen bonds of which four are intramolecular between resorcinol moieties. The mentioned intermolecular motifs involving hosts, neutral diamines and MeOH molecules create infinite chains in [321] direction with repetitive **4**(A)-$[\mathbf{2}-H]^-$-MeOH-**4**(B)-MeOH-$[\mathbf{2}-H]^-$– sequences. On the other hand the O–H···N hydrogen bonds between the host and diamine A molecules also leads to the formation of pseudo-capsular chains in *ab* plane interlinked by diamine A molecules (Fig. 7b). The third intermolecular hydrogen bond donated by the host, connects the host molecules (and pseudo-capsules) with parallel side-by-side fashion leading to the formation of similar infinite chains (along *a* axis) as in structures **I** and **II**. The phenolate oxygen atom of the host is similarly accepting three hydrogen bonds (Table 2).

Solution studies were done through a series of ^{1}H NMR titration experiments between the hosts **1**-**2** and the diamine **4** in acetone-d_6 at 303 K. In the experiments, increasing amounts of the diamine **4** was added to a solution of each of the resorcinarene host **1** or **2**. Deprotonation of the resorcinarene –OH groups was observed by the disappearance of the signals upon the addition of the diamine **4** (Fig. ESI). New signals corresponding to the protonated diamine was observed. Downfield shifts of the diamine -CH_2 and -CH_3 signals were observed and it is attributed to the protonation of the diamine (See ESI).

The effect of the amines **3**-**4** on the resorcinarenes in the gas phase was studied through a series of electrospray ionization mass spectrometric analyses. In each experiment, an equimolar mixture of the amine and the resorcinarene were mixed, electrosprayed and analysed in the positive and negative ion modes. Taking the mixture of the diamine **4** and resorcinarene **1** as an example, in the positive ion mode, a monomeric 1:1 complex ($[\mathbf{1}\bullet\mathbf{4}+H]^+$ *m/z* 715) and dimeric ($[\mathbf{1}_2\bullet\mathbf{4}+H]^+$ *m/z* 1315) complexes were observed (Fig. 8a). This result complements observation in the solid state. In the negative ion mode, a deprotonated resorcinarene monomer ($[\mathbf{1}-H]^-$ *m/z* 599) and dimer ($[\mathbf{1}_2-H]^-$ *m/z* 1199) were also observed (Fig. 8b). In the absence of solvent in the gas phase, the deprotonated oxygen will readily form a strong intermolecular hydrogen bond with a neighbouring hydroxyl group of a second resorcinarene molecule resulting to the dimeric assembly. The isotope patterns obtained by experiment agree with those simulated on the basis of natural abundances. Samples containing other combinations of the resorcinarene hosts **1**-**2** and the tertiary amines **3**-**4** were measured and analysed (see ESI) with results showing similar patterns as observed in Fig. 8.

Conclusion

The present work reports interesting supramolecular features resulting from the deprotonation of two resorcinarenes **1**-**2** by mono- and diamines **3**-**4**. The deprotonation of the resorcinarenes results in a net negative charge of the macrocycle which results in enhanced intermolecular hydrogen bonding with neighbouring resorcinarenes forming a diverse array of self-assembled architectures. The protonated amines subsequently acts as guests and nicely fit into the bowl cavities of the resorcinarenes through cation···π and C–H···π interactions forming 1:1 inclusion complexes and 2:1 pseudo-capsular assemblies in the solid state. The deprotonating of the resorcinarenes were also observed in solution via ^{1}H NMR titration studies. The deprotonated resorcinarenes (monomer and dimer) were observed in the negative ion mode while the 1:1 and 2:1 complexes with the protonated amines were observed in the positive ion mode in the gas phase. This work contributes to our understanding of the complex nature of events that occur when amines are used as bases in compounds containing phenolic hydroxyl groups in general and in resorcinarene chemistry in particular.

Acknowledgements

We gratefully acknowledge the Academy of Finland (KR: grant no. 265328, and 263256, NKB: grant no. 258653,) and the University of Jyväskylä (KR) and the Tampere University of Technology (AV) for financial support.

Experimental

The resorcinarene hosts **1**-**2** were synthesized according to reported procedures.[4] The amines **3**-**4** were commercially available. The mass spectrometric experiments were performed with a Micromass LCT Electrospray ionization–Time-of-flight instrument equipped with a Z geometry electrospray ion source. For the experiment, the samples were introduced into the source as acetone solution mixtures at flow rates of 10 µl/min, source temperature of 80 °C and a dissolvation temperature of 120 °C. Multiple scans were recorded and averaged for each spectrum in order to improve the signal-to-noise ratio. Titration experiments were carried out in Acetone-d_6 at 303 K on a Bruker Avance DRX 500 MHz. Solutions of host **1**-**2** was treated with various amounts of the diamine **4**. The single crystals suitable for structure determination by X-ray diffraction experiments were

obtained by slow evaporation of the samples in loosely closed test tubes. The structural data for **I** and **II** were collected with Agilent SuperNova dual wavelength diffractometer, using micro-focus X-ray source and multilayer optics monochromatized CuKα radiation. The data collection, reduction and multi-scan absorption correction were made by program CrysAlisPro.[39] The data for **III** were collected with Bruker-Nonius KappaCCD diffractometer (APEX-II detector), using graphite monochromatized MoKα radiation. The data collection was performed with Collect[40], data reduction with Denzo-SMN[41] and absorption correction with Sadabs[42] software. The structures were solved by direct methods, using SIR-2011,[43] and refined on F^2 using SHELXL-97.[44] The hydrogen atoms bonded to C atoms were treated with riding model. The O–H and N–H hydrogens are found from electron density maps and refined by restraining the O–H (0.84 Å) and N–H (0.91 Å) distances, as well as, by setting U_{iso}(H) factors equal to 1.5 (O-H) and 1.2 (N-H) times the parent atom factor. Crystallographic parameters are collected in Table 1. The thermal ellipsoids (50% probability) diagrams were drawn with ORTEP-3[45] and are presented in ESI.

Notes and references

[a] *Department of Chemistry, University of Jyvaskyla, P. O. Box 35, 40014 Jyvaskyla, Finland. Fax: +358-14-260-2652; E-mail:* kari.t.rissanen@jyu.fi, ngong.k.beyeh@jyu.fi
https://www.jyu.fi/kemia/tutkimus/orgaaninen/en/research/rissanen
[b] *Department of Chemistry and Bioengineering, Tampere University of Technology, P. O. Box 541, 33101 Tampere, Finland; E-mail:* arto.valkonen@tut.fi

† Electronic Supplementary Information (ESI) available: Crystal structures, crystallographic data CCDC numbers 969816- 969818. ^{1}H NMR titration spectra and mass spectra. See DOI: 10.1039/b000000x/

‡ Footnotes should appear here. These might include comments relevant to but not central to the matter under discussion, limited experimental and spectral data, and crystallographic data.

1 J.-M. Lehn, *Pure Appl. Chem.,* 1994, **66**, 1961.
2 J.-M. Lehn, *Supramolecular Chemistry: Concepts and Perspectives*, 1995.
3 G. R. Desiraju, *Angew. Chem., Int. Ed. Engl.,* 1995, **34**, 2311.
4 P. Timmerman, W. Verboom and D. N. Reinhoudt, *Tetrahedron,* 1996, **52**, 2663.
5 V. Böhmer, *Angew. Chem. Int. Ed. Engl.,* 1995, **34**, 713.
6 K. Rissanen, *Angew. Chem., Int. Ed.,* 2005, **44**, 3652.
7 J. L. Atwood, L. J. Barbour and A. Jerga, *Chem. Commun.,* 2001, 2376.
8 N. K. Beyeh and K. Rissanen, *Isr. J. Chem.,* 2011, **51**, 769.
9 S. Busi, H. Saxell, R. Fröhlich and K. Rissanen, *CrystEngComm,* 2008, **10**, 1803.
10 T. Gerkensmeier, W. Iwanek, C. Agena, R. Fröhlich, S. Kotila, C. Näther and J. Mattay, *Eur. J. Org. Chem.,* 1999, **1999**, 2257.
11 H. D. F. Winkler, E. V. Dzyuba, J. A. W. Sklorz, N. K. Beyeh, K. Rissanen and C. A. Schalley, *Chem. Sci.,* 2011, **2**, 615.
12 H. Mansikkamäki, M. Nissinen and K. Rissanen, *Chem. Commun.,* 2002, 1902.
13 M. M. Conn and J. J. Rebek, *Chem. Rev.,* 1997, **97**, 1647.
14 J. Kang and J. Rebek, *Nature,* 1996, **382**, 239.
15 H. Mansikkamäki, M. Nissinen and K. Rissanen, *CrystEngComm,* 2005, **7**, 519.
16 N. K. Beyeh, M. Kogej, A. Åhman, K. Rissanen and C. A. Schalley, *Angew. Chem., Int. Ed.,* 2006, **45**, 5214.
17 H. Mansikkamäki, M. Nissinen and K. Rissanen, *Angew. Chem., Int. Ed.,* 2004, **43**, 1243.
18 H. Mansikkamäki, S. Busi, M. Nissinen, A. Åhman and K. Rissanen, *Chem. Eur. J.,* 2006, **12**, 4289.
19 M. Yamanaka, A. Shivanyuk and J. J. Rebek, *J. Am. Chem. Soc.,* 2004, **126**, 2939.
20 L. Avram and Y. Cohen, *J. Am. Chem. Soc.,* 2002, **124**, 15148.
21 D. Braga, *Chem. Commun.,* 2003, 2751.
22 A. Corma, S. Iborra, I. Rodriguez, M. Iglesias and F. Sanchez, *Catal. Lett.,* 2002, **82**, 237.
23 F. Csende, F. Miklos and A. Porkolab, *Curr. Org. Chem.,* 2010, **14**, 745.
24 M. Kanai, N. Kato, E. Ichikawa and M. Shibasaki, *Pure Appl. Chem.,* 2005, **77**, 2047.
25 V. Khedkar, A. Tillack, C. Benisch, J. Melder and M. Beller, *J. Mol. Catal. A: Chem.,* 2005, **241**, 175.
26 C. Perego and D. Bianchi, *Chem. Eng. J.,* 2010, **161**, 314.
27 D. D. Cram, M. T. Blanda, K. Paek and C. B. Knobler, *J. Am. Chem. Soc.,* 1992, **114**, 7765.
28 D. J. Cram, *Science,* 1983, **219**, 1177.
29 A. Jasat and J. C. Sherman, *Chem. Rev.,* 1999, **99**, 931.
30 J. R. Moran, S. Karbach and D. J. Cram, *J. Am. Chem. Soc.,* 1982, **104**, 5826.
31 N. K. Beyeh, J. Aumanen, A. Åhman, M. Luostarinen, H. Mansikkamäki, M. Nissinen, J. Korppi-Tommola and K. Rissanen, *New J. Chem.,* 2007, **31**, 370.
32 M. Luostarinen, M. Nissinen, M. Nieger, A. Shivanyuk and K. Rissanen, *Tetrahedron,* 2006, **63**, 1254.
33 M. Nissinen, E. Wegelius, D. Falabu and K. Rissanen, *CrystEngComm,* 2000, 28.
34 S. Zheng, M. Gembicky, M. Messerschmidt, P. M. Dominiak and P. Coppens, *Inorg. Chem.,* 2006, **45**, 9281.
35 K. Murayama and K. Aoki, *Chem. Commun.,* 1998, 607.
36 J. L. Atwood, L. J. Barbour, M. J. Hardie, E. Lygris, C. L. Raston and H. R. Webb, *CrystEngComm,* 2001, **3**, 41.
37 V. A. Pankratov, T. M. Frenkel, A. E. Shvorak, S. V. Lindeman and Y. T. Struchkov, *Russ. Chem. B+.,* 1993, **42**, 81.
38 A. Shivanyuk, K. Rissanen and E. Kolehmainen, *Chem. Commun.,* 2000, 1107.
39 *CrysalisPro*, version 1.171.36.28; Agilent Technologies: Oxford, UK, 2013.
40 COLLECT, Bruker AXS Inc.: Madison, Wisconsin, USA, 2008.
41 Z. Otwinowski and W. Minor, *Methods in Enzymology*, Academic Press, New York, 1997.
42 G. M. Sheldrick, *University of Göttingen, Göttingen, Germany,* 2008.
43 M. C. Burla, R. Caliandro, M. Camalli, B. Carrozzini, G. L. Cascarano, C. Giacovazzo, M. Mallamo, A. Mazzone, G. Polidori and R. Spagna, *J. Appl. Crystallogr.,* 2012, **45**, 357.
44 G. M. Sheldrick, *Acta Crystallographica Section A,* 2008, **64**, 112.
45 L. J. Farrugia, *J. Appl. Crystallogr.,* 2012, **45**, 849.

The deprotonation of a resorcinarene by a small organic bases results in 1:1 inclusion and 1:2 pseudo-capsular ion-pair complexes.